Electron Energy Loss Spectral Imaging of TiC formed by Supernovae: A Scanning Transmission Electron Microscopy Study of Grain Formation and Alteration Mechanisms. T. L. Daulton[1,2], T. J. Bernatowicz[2,3], and T. K. Croat[2,3], [1]Center for Materials Innovation, [2]Physics, [3]Laboratory for Space Sciences, Washington University in St. Louis, St. Louis MO 63130, USA.

Introduction:

Primitive carbonaceous chondrites contain within their matrices micron-sized spherules of presolar graphite [1]. In Murchison, graphite spherules of supernovae (SN) origin have a mean diameter of ~ 6 μm and a relatively low density (1.65-1.72 g/cm^3), while those of asymptotic giant branch (AGB) star origin are smaller (mean diameter of ~ 2 μm) and a higher density (2.15-2.20 g/cm^3) [2]. Embedded within the graphite spherules are 7-500 nm TiC grains (often in solid solution with V, Zr, Mo, Ru, and N with combined solute atom concentrations ~ < 20 at.%) that were undoubtedly incorporated during graphite condensation [2-6]. While both AGB and SN graphite spherules contain TiC, only TiC grains from supernovae are associated with 10-80 nm diameter Fe-Ni metal kamacite and taenite grains, usually found epitaxially grown on their surface. The measured mass abundances of carbide and metal subgrains in SN graphites range from 25-2400 ppm (corresponding to 1-1000 subgrains per spherule).

These high-temperature condensates were ubiquitous in their respective gas outflows at regions of graphite formation, and their microstructures record valuable information on chemical and physical conditions present within the relatively short interval between their formation and subsequent encapsulation [2]. Once shielded within the interior of the graphite spherules, these subgrain microstructures survived largely unaltered, protected from subsequent chemical processing in the interstellar media and solar nebula.

Specimens & Methods:

Graphite spherules (KEe6, KEe15) from the Murchison KE3 density separate that exhibited isotopic anomalies characteristic of SN origin {^{16}O/^{18}O (290 ± 12, 236 ± 9); ^{12}C/^{13}C (231 ± 2, 59.7 ± 0.3); δ^{29}Si (-1 ± 32 ‰, 11 ± 63 ‰); and δ^{29}Si(-11 ± 32 ‰, 93 ± 59 ‰), respectively} [1] were ultramicrotomed [5] for scanning transmission electron microscopy (STEM).

Elemental (C, Ti, V, O, N, and Fe) maps were acquired by STEM- electron energy loss spectroscopy (EELS) spectral imaging using a JEOL JEM-2100F instrument equipped with a Tridiem Gatan imaging filter (GIF). A GIF spectrometer 5 mm diameter entrance aperture, a collection angle of 2β = 22.66 ± 0.06 mrad, and an energy dispersion of 0.3 eV/channel were used. Spectral images were acquired by collecting EELS spectra at each pixel position within a STEM region of interest that contained ≈ 14 k pixels. The spectra were corrected for dark current and channel-to-channel gain variation of the CCD detector array and collected in the diffraction mode of the microscope (i.e., image coupling to the EELS spectrometer). Core-loss and low-loss EELS spectral images were collected in serial. Raster dwell times were 0.02 s per pixel (~ 2 hrs per image acquisition, due to CCD readout-limited acquisition) and 3 - 4 s per pixel (12 - 15 hrs per image acquisition) for the low-loss and core-loss spectral images respectfully. Background subtraction is critical and non-trivial for quantification of the EELS adsorption edge signals. At each pixel position in a core-loss spectra image, power-law backgrounds were carefully fit to each pre-edge region and subtracted from the respective EELS adsorption edge. Plural scattering was removed by Fourier deconvolution of the core-loss spectra with the corresponding low-loss spectra after spatial alignment of the two spectral images. Ratios of integrated EELS core-loss signal between elements were converted to their corresponding atomic ratios using partial cross-sections that were calculated from theoretical Hartree-Slater models. Unlike maps of EELS core-loss signal, maps of relative elemental compositions are, in principle, not influenced by variations in specimen thickness and electron diffraction.

Results & Discussion:

Here we report further results of our on-going study. In bright-field and high angle annular dark-field STEM images, most TiC grains displayed some evidence of (3 - 5 nm thick) rims on their surface. We have previously shown that these rims possess a highly disordered atomic structure [6]. Visibility of the rims is proportional to the level of atomic disorder present and the grain population likely exhibits a distribution in the level of disorder at grain surfaces. The presence of disordered rims suggests post formation alteration in the SN outflows. Two possible mechanisms for rim formation are a) particle irradiation due to collisions between grains and gas moving at different relative velocities (reminiscent of rim formation on lunar soil grains by solar wind) and b) chemical corrosion from exposure to reactive gas species following grain growth [4,5].

Five rimmed, one partially rimmed, and one apparently non-rimmed TiC grains were mapped with STEM-EELS. The TiC grains exhibit heterogeneous, mottled V compositions (see Fig. 1). The mean V composition of a grain ranges from 4-12 at.%, consistent with previous energy dispersive X-ray spectroscopy measurements [5]. In some TiC grains, readily discernible enrichments of V are localized in distinct surface regions. Clearly identifiable radial (core to surface) gradients in V composition have not yet been observed. Enrichments of O at the surface ~ < 20 at.% (continuous across the entire surface, e.g. see Fig. 1, or sometimes localized in distinct surface regions) were also observed. It is reasonable to assume that the O enrichments are not an oxidation artifact from specimen isolation in the laboratory by acid dissolution. Previous nanoSIMS measurements of 11 TiC grains contained in the KE3e10 SN graphite spherule showed that all exhibited $^{16}O/^{18}O$ isotopic anomalies, which in most cases exceeded those of the host graphite [7]. The TiC grains have N distributed relatively uniformly in the bulk with mean grain compositions raging between ≈ 0 - 10 at. %. Further, some grains display N enrichments at the surface (continuous across the entire surface, e.g. see Fig 1, or sometimes localized in discrete surface regions).

Six of the seven TiC grains that were mapped (four rimmed, one partially rimmed, and the apparently non-rimmed) exhibited enrichments of V, O, and/or N at their surfaces. Four of the TiC grains had Fe-rich grains on their surface and the largest of these (50 nm diameter) exhibited a disordered surface rim. Elevated concentrations of chemically diverse elements V, O, and N at TiC grain surfaces, and the presence of disordered rims on chemically diverse mineral grains TiC and Fe-Ni kamacite/taenite suggest a chemically independent mechanism such as ion implantation for the surface modification of these grains. The presence of high densities of lattice defects in TiC at and in proximity to their rims [6] further supports an implantation mechanism.

References: [1] Amari S. et al. (1994) *Geochim. Comoschim. Acta*, 58, 459-470. [2] Bernatowicz T. J. et al. (2006) in *Meteorites and the Early Solar System II*, eds D. Lauretta & H. Y. McSween Jr., (U. of Arizona Press), 109-126. [3] Bernatowicz T. J. et al. (1991) *Astrophys. J.*, 373, L73-L76. [4] Bernatowicz T. J. et al. (1999) *LPSC XXX*, 1392. [5] Croat T. K. et al. (2003) *Geochim. Comoschim. Acta*, 67, 4705-4725. [6] Daulton T. L. et al. (2009) *LPSC XL*, 1996. [7] Stadermann F. J. et al. (2005) *Geochim. Comoschim. Acta*, 69, 177-188.

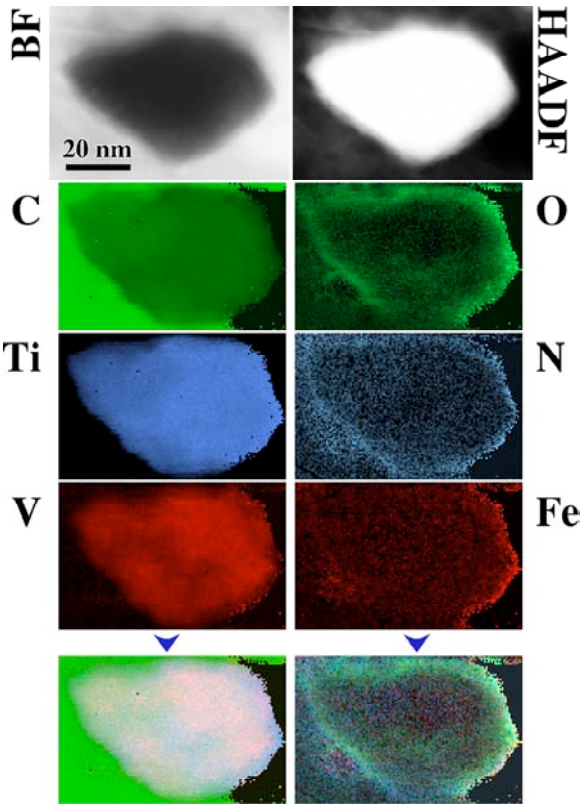

Fig. 1. Bright field (BF) and high angle annular dark field (HAADF) images of a typical rimmed supernovae TiC grain. Electron energy loss spectroscopy acquired compositional maps (color panels) show enrichment of O, N, and possibly Fe at the (≈ 5 nm thick) surface of the grain relative to bulk as well as a heterogeneous V composition. Note, the color ranges for each elemental map are not normalized between 0 at.% and 100 at.% (see Fig. 2), and have been independently adjusted to enhance visual clarity (consequently they are not directly comparable).

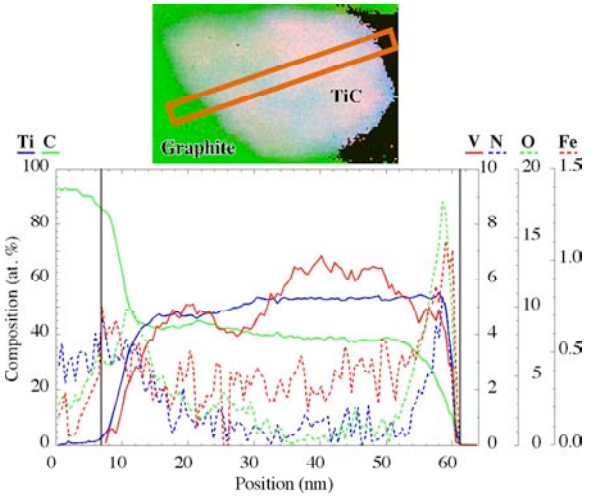

Fig. 2. Column-averaged compositional profile plots across a region of interest (orange rectangle) within the TiC of Fig. 1. Vertical lines depict the extent of the grain.